



AENSI Journals

Australian Journal of Basic and Applied Sciences

ISSN:1991-8178

Journal home page: www.ajbasweb.com



Performance Evaluation of Brushless Exciter for Aircraft Applications

¹Deepak Arumuagm and ²Premalatha Logamani
Deepak Arumuagm

¹Research scholar, Department of Electrical and Electronics Engineering, Anna University, Chennai, India-600025.

²Professor & head, Department of Electrical and Electronics Engineering, Anand Institute of Higher Technology, Chennai, India.

ARTICLE INFO

Article history:

Received 10 October 2014

Received in revised form

22 November 2014

Accepted 28 November 2014

Available online 1 December 2014

Keywords:

Aircrafts, multi stage generator system, Inverted synchronous generator, finite element analysis

ABSTRACT

Background: In general the main generator in multistage generator system takes an input current for field windings from brushless exciter (or) Inverted synchronous generator through rotating rectifier. This multistage generator system provides power supply to the Aircrafts during emergency period. So, it is necessary to study & analyze the performance of brushless exciter for high speed applications. **Objective:** To perform magnetic field analysis and Thermal analysis of brushless exciter for high speed applications. **Results:** The analytical design using classical design equations and FEM based simulation results such as flux linkage, voltage, current and heat flow of 262W/9000rpm brushless exciter presented and compared. **Conclusion:** We have designed a brushless exciter for high speed application using standard mathematical expressions analytically. The theoretically designed parameters implemented in the finite element software's such as MagNet and ThermNet. Finally the overall performance of the simulated machine compared with the analytical design values.

© 2014 AENSI Publisher All rights reserved.

To Cite This Article: Deepak Arumuagm and Premalatha Logamani., Performance Evaluation of Brushless Exciter for Aircraft Applications. *Aust. J. Basic & Appl. Sci.*, 8(18): 151-158, 2014

INTRODUCTION

In modern aircrafts, 30W-250kW power system provides power supply to the lighting load, Gunshots, Cockpit and other loads. If this power system fails, the multistage generator system comprising of three generators will act as a backup system to provide continuous power supply to the emergency loads. They are Permanent Magnet Synchronous Generator (PMSG), Inverted Synchronous Generator (ISG) (or) Brushless Exciter (BE) and Synchronous Generator. This generator system gets the mechanical input from the aircraft engine through the Aircraft mounted auxiliary gear box (AMAGB). Three integrated machines are connected at a common shaft in this generator system (Roy Perryman, 2006; Nicolas Patin, 2008; Ashraf Tantawy, 2008; Navedtra, 2002). In general the speed of modern aircraft generators lies from 7000rpm to 24000rpm while the traditional civil aircrafts have two main distribution power busses such as high power 3 Φ , 115V Ac, 400Hz and low power 28V DC (Ahmed Abdel-Hafez, 2012).

Excitation systems are one of the most important parts of the synchronous generators. According to the excitation source used excitation systems are classified as DC systems and AC systems. DC excitation systems utilize direct current generators. In such systems direct current is provided to the rotor of the synchronous generator through the slip rings. The AC excitation system utilises an AC generator as the system exciter. This system is divided into stationary and rotating AC rectifier systems. In stationary rectifiers the DC output is fed to the field winding of the generator through the slip rings. On the contrary, in rotating rectifiers DC is directly fed to the generator field as the armature of the exciter and rectifiers rotate with the generator field. Such systems are known as brushless systems and were developed to avoid the problems with brushes when extremely high field currents of large generators are applied (Peter Butros, 2011). This system has more reliability, eliminate carbon brushes, slip rings, carbon dust and maintenance cost.

The conventional methods of design are based on the assumed flux path method for the determination of flux distribution inside the machines. They use analytical formulae that are based on lumped parameters estimation using linear magnetic circuit model. The machine is assumed to have infinitely deep rectangular slots and the core of the machine is operated under unsaturated conditions. These assumptions may not be suitable for the latest design of electrical machines with complex geometries and non-linearity. Due to the accuracy and accessibility, FEM (Finite Element Method) is widely used in the design and analysis of all types of electrical machines. The development of FEM improves the structural mechanics community serving the aircraft industry

Corresponding Author: Deepak Arumuagm, Research scholar, Department of Electrical and Electronics Engineering, Anna University, Chennai, India-600025.

(Antonio Griffo, 2013; Shinya Matsutomo, 2006; J Tinsley Oden, 2004; Alejandro B. Díaz-Morcillo, 2002). Based on the FEM, electromagnetic and thermal analysis of the machine is carried out. In (C W Trowbridge, 2006) the finite element analysis of 225KVA/230V brushless exciter for aircraft application was discussed using 2D analysis. Also nonlinear analysis and end winding effects of starter generator was presented using 3D analysis. The various types of design, magnetic field analysis, Thermal effects and losses are analysed using finite element software's for different applications was presented in (Fang deng, 1998; Julio-César Urresty, 2010; M.A.Arjona L, 1999; Zlatko Kolondzovski, 2005; Chang Eob Kim, 2002; H. Yaghibi, 2011; Sami Ruoho, 2007; B.Jagadeesh Chandra Prasad, 2011)

In this paper, the entire model of 262W/26.2V Brushless Exciter (BE) (or) Inverted synchronous generator (ISG) is designed theoretically. The Electromagnetic and Thermal analyses of Inverted synchronous generator are carried out using the software of 2D-transient finite element analysis. At last, the overall performance of the machine is compared with the analytical design at a speed of 9000rpm. The organization of the paper is as follows: Section II deals with description of multistage generator system while analytical design of inverted synchronous generator has been discussed in section III. The simulation results of inverted synchronous generator are given in section IV. The comparison between theoretical and simulation results are presented in section V, while section VI is the conclusion.

System Description:

The overall structure of the Hybrid excitation system is shown in Fig 1. The Hybrid excitation system comprises of 3 integrated machines. They are Permanent Magnet Generator (PMG), Inverted synchronous Generator (ISG) or Brushless exciter and Main Generator (MG). All the three machines are mounted on a single shaft and connected to the aircraft engine through a gear box [2, 3]. The AC output voltage of PMG is rectified by Generator control unit (GCU) and then this rectified constant DC voltage is applied to field windings of the main exciter. The output voltage of the main generator is regulated through Main Exciter. At last, 28V DC output voltage is connected to an emergency DC load bus with the help of 12 pulse rectifier circuits. The generator is incorporated with forced air cooling and operates in high speed envelope, high ambient temperature and handles very high current.

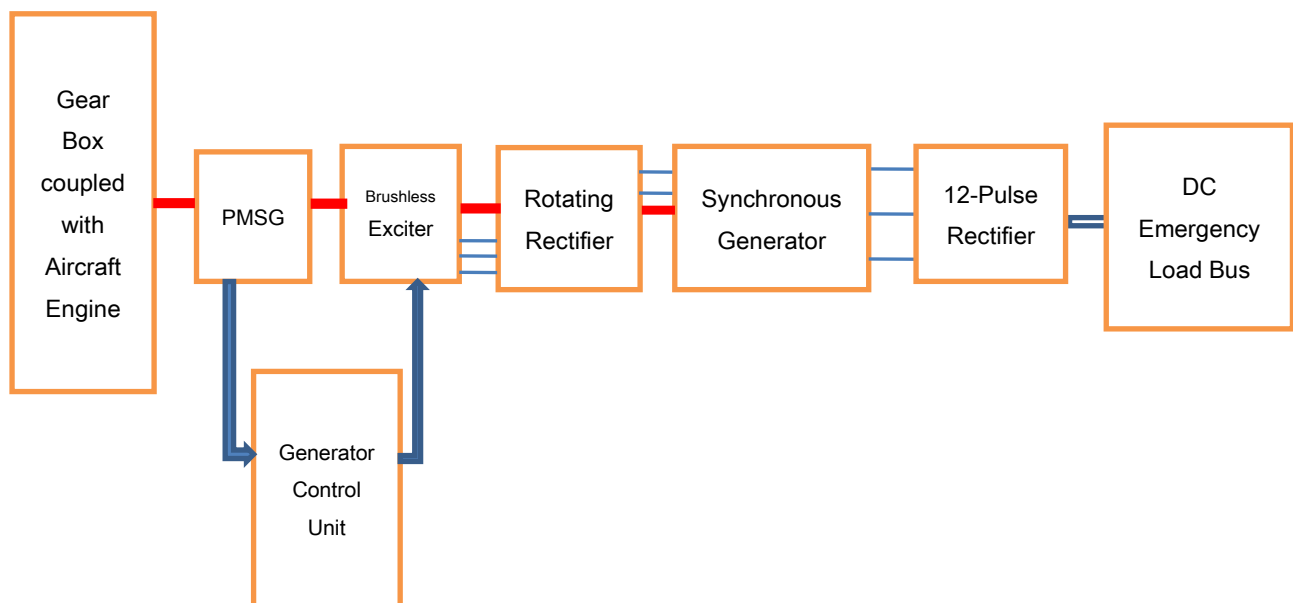


Fig. 1: General Structure of the Multi Excitation System.

Analytical Design of Inverted Synchronous Generator / Brushless Exciter:

The ISG is designed by applying standard design expression available in the literature. The rotor reference frame steady-state equations of a field-excited synchronous machine modelled with one q-axis, a field and one damper winding in the d-axis is

$$V_{qs} = i_{qs} r_s + i_{ds} X_{ds} + (i_{dr} + i_{fr}) X_{md} \quad (1)$$

$$V_{ds} = i_{ds} r_s - i_{qs} X_{qs} + i_{qr} X_{mq} \quad (2)$$

$$V_{fr} = i_{fr} R_{fr} \quad (3)$$

The output RMS current is given by

$$I_s = \sqrt{i_{qs}^2 + i_{ds}^2} \quad (4)$$

KVA rating of a 3 phase synchronous machine is

$$KVA = 11 K_{w1} B_{avg} q D^2 L n_s * 10^{-3} \quad (5)$$

Where

K_{w1} = winding factor for stator winding

B_{avg} = Specific Magnetic Loading

q = Specific Electric Loading

D = Diameter of stator bore

n_s = Synchronous speed in rps

Induced EMF per phase of the of a synchronous machine is

$$E_{ph} = 4.44 K_{w1} \Phi_m f T_{ph} \text{ in Volts} \quad (6)$$

Where

Φ_m = Maximum flux passing through the core

f = frequency in Hz

T_{ph} = Total number of turns per phase

$$\text{Specific Magnetic Loading} \quad B_{av} = \frac{p \Phi_m}{\pi D L} \quad (7)$$

$$\text{Area of the stator Conductor} = a_1 = \frac{I_{ph}}{A \delta} \quad (8)$$

Where

δ = current density

A = Number of parallel paths

I_{ph} = stator current per phase

Slot width b_{ss} = Width of bare conductor + (Insulation over conductor * Number of conductors along with of slot) + slot liner thickness + Clearance (9)

Depth of Slot = h_{is} = Depth of bare conductor + (Insulation over conductor * Number of conductors along depth of slot) + (Number of micanite strip * Thickness of strip) + Thickness of micanite separator + Thickness of slot liner (10)

Flux density in the stator core

$$B_{cs} = \frac{\phi_m / 2}{d_{cs} L_i} \quad (11)$$

Depth of stator core

$$d_{cs} = \frac{\phi_m / 2}{B_{cs} L_i} \quad (12)$$

External diameter of the stator stampings

$$D_o = (D + 2 h_{ts} + 2 d_{cs}) \quad (13)$$

Length of mean turn of the stator conductors

$$L_{mt} = (2L + 2.5 \tau + \text{overhang} + 20) \quad (14)$$

Resistance of the stator winding per phase

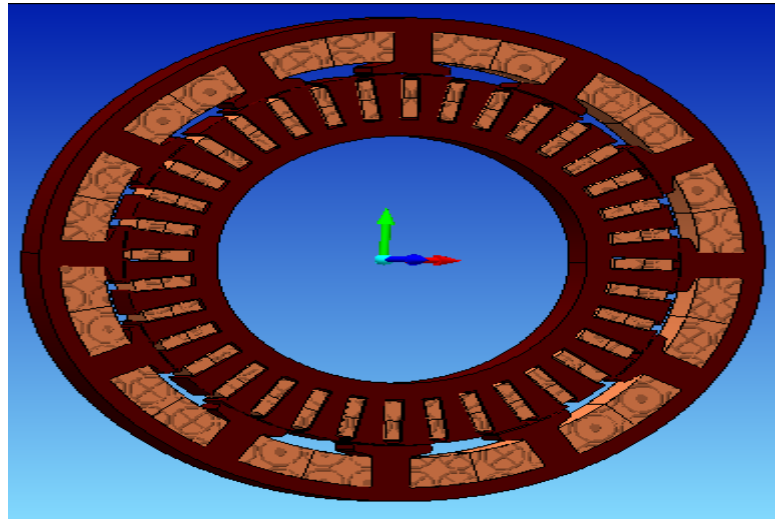
$$R_1 = \frac{\rho L_{mt}}{a_1} T_1 \quad (15)$$

The machine has been designed to meet the power output specifications for an aircraft. The specifications of such a design are listed in Table 1.

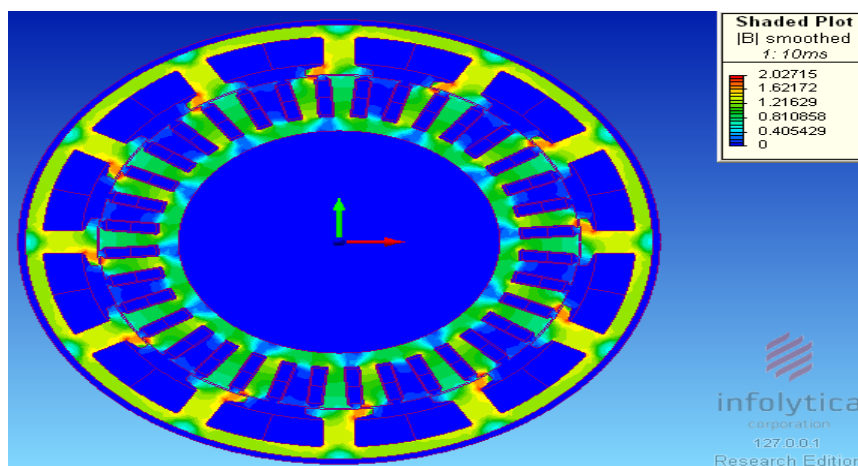
The FEM model of designed ISG is shown if Fig 2. The ISG has 12 stator slots and 36 rotor poles, as shown in (Fig 2). The stator has Field winding and the rotor carries concentric windings. The main advantage of this structure is to eliminate slip rings and brushes.

Table 1: Parameters of the ISg.

S.No	Parameters	Values
1	Rated Power, (W)	262
2	Rated DC Voltage, V_{dc} (V)	26
3	Phase Current, I_{ph} (A)	7.4
4	Stator Outer Diameter, ods (mm)	106.2
5	Rotor Outer Diameter, odr (mm)	71
6	Length of the Air gap, L_g (mm)	6
7	Speed, N (rpm)	9000
8	Number of Rotor Slots, S	36
9	Number of Stator Poles, P	12
10	Power Factor	0.88
11	Flux/Pole, (k_{Max})	3.78

**Fig. 2:** Cross Sectional View of ISG.**Simulation Analysis of Brushless Exciter:**

In the finite element method, a given system is divided into finite elements called meshes and an approximate solution of the problem is developed in each phase. This method allows accurate representation of complex geometrics & inclusion of dissimilar materials. It enables accurate representation of the solution within each element to bring out all local effects. The design parameters evaluated in section 3 is modeled and simulated in the FEM environment using MagNet and ThermNet packages.

**Fig. 3:** Magnetic Flux Distribution during no load at 9000rpm.**Magnetic Field Analysis of ISG:**

The electromagnetic analysis of the machine is carried out using the MagNet software. In the pre-processor analysis, the model of the machine is developed and all its parts are modeled with by assigning the appropriate

materials based on the values evaluated using the conventional design procedures. The core of both stator and rotor are made up of coldrolled steel and windings are made up of copper.

In the post-processor analysis, the magnetic flux distribution of the machine under no-load condition can be obtained as shown in Fig 3. It is very evident from figure, that the flux density in the core of the machine is uniformly distributed. The maximum value of the flux density is 2.02 Wb/m^2 at 9000rpm which shows the results obtained using simulation is much closer to the values obtained from theoretical analysis. The flux density is maximum at the edges of the poles. The leakage flux of the machine is negligible as depicted by the results of simulation.

The induced three phase voltage waveforms of the ISG under no-load condition at 9000rpm are shown in the Fig 4. From the plot of the voltage waveform, it is observed that the induced voltage is sinusoidal and the maximum voltage at no load condition is 26V at 9000rpm. The value of the induced voltages obtained using simulation closely correlates with the theoretical values.

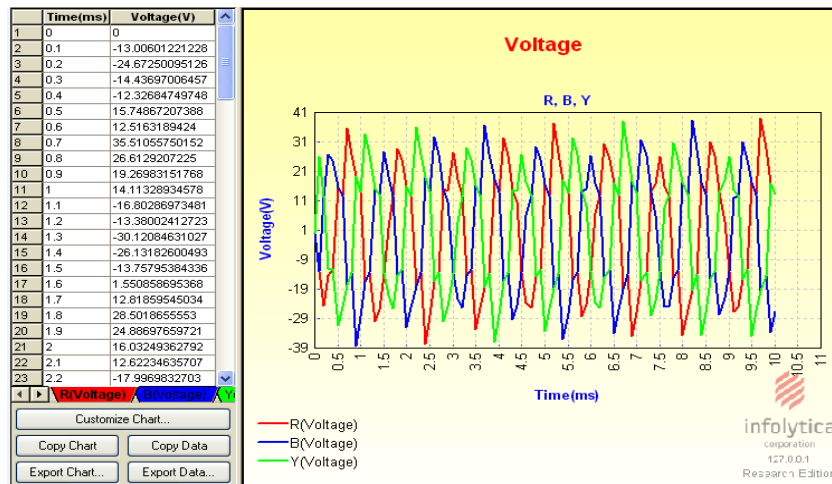


Fig. 4: Voltage on no load condition at 9000rpm.

The current flowing through the armature windings under no-load condition is shown in Fig 5. It is very clear, that the current through the stator coils are balanced and it is sinusoidal. The average value of current is 18A.

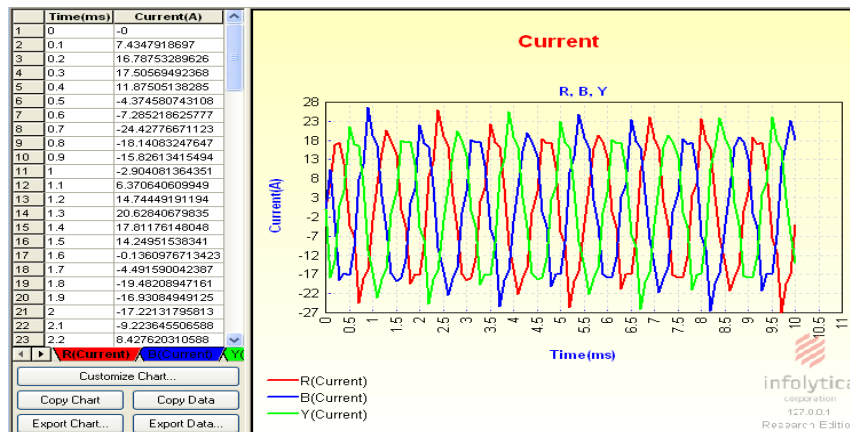


Fig .5: Current through the armature windings.

The output of the ISG is connected to a pure resistive load through a three-phase diode bridge rectifier. A load of 3.5Ω is connected to the rectifier output provided with capacitor filter. The maximum DC voltage that is obtained across the load is 22V at 9000rpm as shown in Fig 6. The maximum DC current that is obtained with the load is 4A at 9000rpm as shown in Fig 7. These values are closely equal to the theoretical values mentioned in the design Table 1.

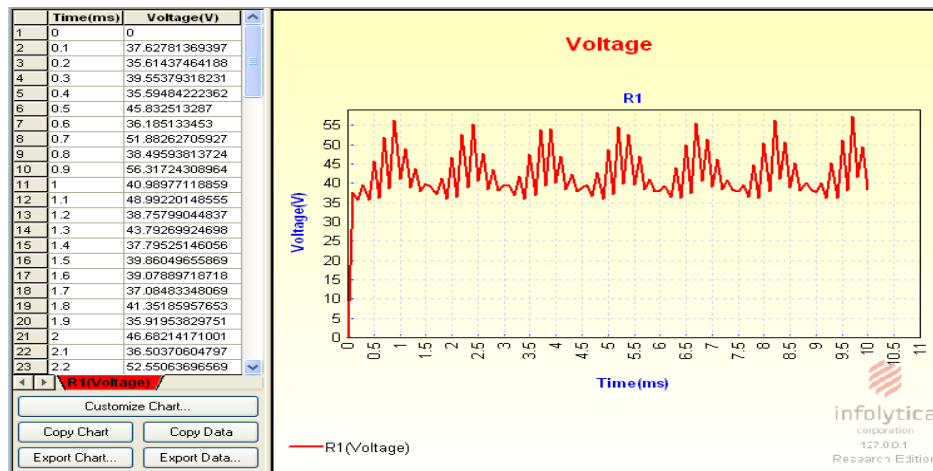


Fig. 6: DC voltage during load condition at 9000rpm.

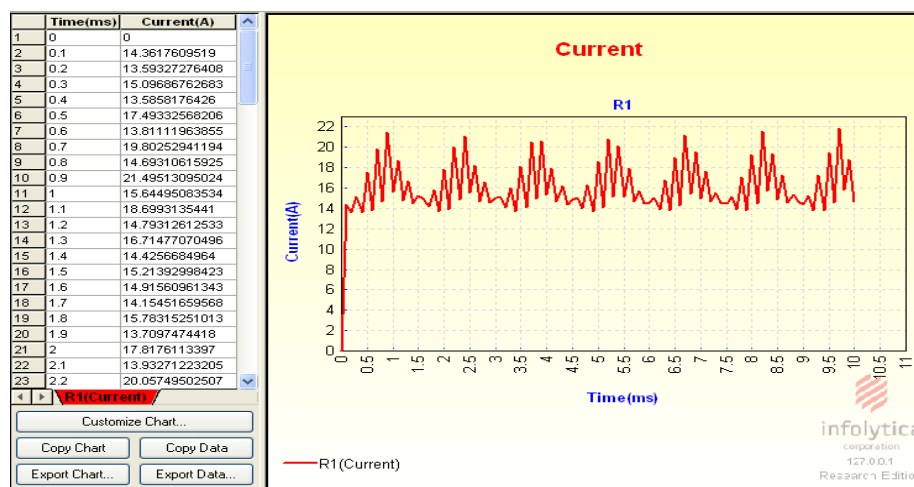


Fig. 7: Load Current at 9000rpm.

Thermal Analysis of ISG:

Thermal analysis of the machine is used to evaluate the heat flow in the machine and the temperature developed in various parts of the machine under dynamic conditions. The analysis is carried out using the ThermNet software and the main source of heat is identified.

In this analysis, the ISG modeled using the MagNet software is directly coupled with the ThermNet software. The total heat generated in the ISG is shown in Fig 8. A maximum temperature of 22.95°C is generated at 9000rpm.

The heat flow inside the ISG at a speed of 9000 rpm is shown in Fig 9. The hot spots of the temperature flow can be located near the edges of the slots. The heat flow rate inside the conductor is nearly zero and it is maximum at the outer periphery of the machine.

Performance Comparison:

The overall performance of ISG has been compared with theoretical and simulation results. The simulation results are compared against various performance parameters such as flux density, induced voltage during no load and load conditions, temperature rise etc. The results of comparison are listed in the table 2.

Table 2: Performance Comparison.

S.No	Parameters of comparison	Theoretical Value	Simulation Value
1	Flux Density at no load (Web/m ²)	2.15	2.02
2	Voltage at no load (V)	26	26
3	DC output Power (W)	262	269
4	Phase current(A)	7.4	7.77
5	Temperature (°C)	24.76	22.95

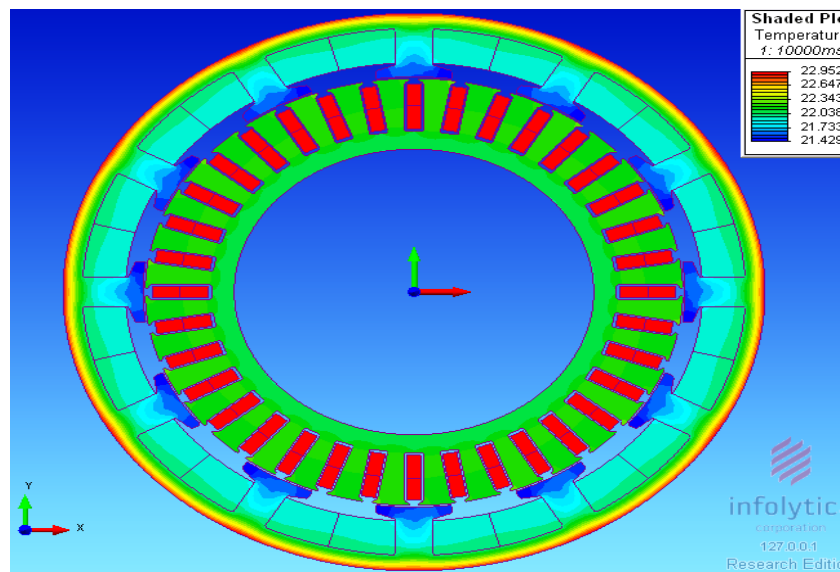


Fig. 8: Temperature distribution in ISG at 9000rpm.

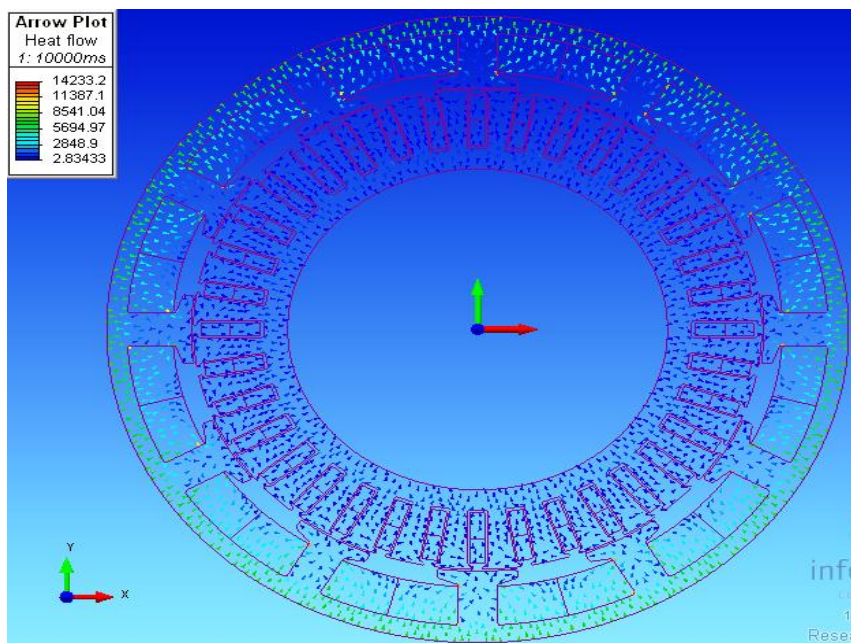


Fig. 9: Total Heat flow at 9000rpm.

From the above table it is prove that, the output voltage, current, flux density and power value obtained from simulation analysis closely matches the values obtained from theoretical design.

Conclusion:

In this work, a 262W/26V ISG has been designed and simulated using MagNet and ThermNet software's. The performance has been evaluated at a speed of 9000rpm for multi stage generator system, which provides efficient and safe operation of the aircrafts. The electromagnetic field analysis of the ISG machine is carried out to determine its magnetic flux density distribution, voltage and current using MagNet software. The temperature and heat flow of the machine is obtained by thermal analysis using ThermNet software. The results of the simulation matches the performance evaluated analytically. It has been proved that the overall performance of the ISG is suitable for high speed conditions envisaged in Aircrafts.

REFERENCES

Ahmed Abdel-Hafez, 2012. Recent advances in aircraft technology, China, In Tech Press.

Alejandro B. Díaz-Morcillo, Juan V. Balbastre, Luis Nuño, 2002. New recovery error indicator for adaptive finite-element analysis on wave guiding structures.

Antonio Griffo, Rafal Wrobel, Phil H. Mellor and Jason M. Yon, 2013. Design And Characterization Of A Three-Phase Brushless Exciter For Aircraft Starter/Generator, IEEE Transactions On Industry Applications, 49(5): 2106-2115.

Arjona, M.A., D.C. Macdonald, 1999. A New Lumped Steady-State Synchronous Machine Model Derived From Finite Element Analysis, IEEE Transactions On Energy Conversion, 14(1): 1-7.

Ashraf Tantawy, Xenofon Koutsoukos, Gautam Biswas, 2008. Aircraft ac generators: hybrid system modeling and simulation, IEEE Conference on Bioengineering, 1-11.

B.Jagadeesh Chandra Prasad, Dr.B.V. Sakker Ram, 2011. Evolution of synchronous Generator Reactance using Finite Element Method, Journal Of Theoretical and Information Technology, 27(2): 68-76.

Chang Eob Kim, J.K. Sykulski, 2002. Harmonic Analysis Of Output Voltage In Synchronous Generator Using Finite-Element Method Taking Account Of The Movement, Ieee Transactions On Magnetics, 38(2): 1249-1252.

Fang deng, Nabeel A. Damerdash, 1998. Comprehensive Salient-Pole Synchronous Machine Parametric Design Analysis Using Time-Step Finite Element-State Space Modeling Techniques, IEEE Transactions On Energy Conversion, 13(3): 221-229.

Julio-César Urresty, Jordi-Roger Riba, Luís Romeral, Antonio Garcia, 2010. A Simple 2-D Finite-Element Geometry for Analyzing Surface-Mounted Synchronous Machines With Skewed Rotor Magnets, Ieee Transactions On Magnetics, 46(11): 3948-3954.

Navedtra, 2002. Aviation electricity and electronics - power generation and distribution, Nonresident Training Course, pp: 1-8.

Nicolas Patin, Lionel Vido, Eric Monmasson, Jean Paul Louis, Mohamed Gabsi, Michel Lecrivain 2008. Control of a hybrid excitation synchronous generator for aircraft applications, IEEE Transactions on Industrial Electronics, 55: 3772-3783.

Paul C. Krause, Oleg Wasynczuk, Scott D. Sudhoff, Analysis of Electrical Machines & drive systems, Wiley Interscience publications, second edition.

Peter Butros, 2011. Simulations of Rotating Brushless AC Excitation System with Controlled Thyristor Bridge Rectifier for Hydropower Generators, Uppsala university, Uppsala.

Roy Perrymam, Landson M.C. Mhango, 2006. High Efficiency High Speed PM Motors for the More Electric Aircraft. Proceedings of the 6th WSEAS International Conference on Power Systems, 368-375.

Sami Ruoho, Emad Dlala, Antero Arkkio, 2007. Comparison Of Demagnetization Models For Finite-Element Analysis Of Permanent-Magnet Synchronous Machines, IEEE Transactions On Magnetics, 43(11): 3964-3968.

Sawhney, A.K., Course in Electrical Machine design, Dhanpat rai & sons publications, fifth edition.

Shinya Matsutomo, Tomoyuki Miyamoto, Kazufumi Kaneda, So Noguchi, Hideo Yamashita, 2006. An error evaluation scheme based on rotation of magnetic field in adaptive finite element analysis, IEEE Transactions on Magnetics, 42: 567-570.

Tinsley Oden, J., Historical comments on finite elements, The University Of Texas at Austin, 125-130.

Trowbridge, C.W., J.K. Sykulski, 2006. Some key developments in computational electromagnetics and their attribution, IEEE Transactions on Magnetics, 42: 503-508.

Yaghobi, H., K. Ansari, H. Rajabi Mashhadi, 2011. Analysis Of Magnetic Flux Linkage Distribution In Salient pole Synchronous Generator With Different Kinds Of Inter turn Winding Faults, Iranian Journal Of Electrical & Electronic Engineering, 7(4): 260-272.

Zlatko Kolondzovski, Lidija Petkovska, 2005. Determination Of A Synchronous Generator Characteristics Via Finite Element Analysis, Serbian Journal Of Electrical Engineering, 2(2): 157-162.